Superconducting properties of very high quality NbN thin films grown by high temperature chemical vapor deposition

D. Hazra[1,2], N. Tsavdaris [3], S. Jebari [1,2], A. Grimm[1,2], F. Blanchet[1,2],

F. Mercier[3], E. Blanquet[3], C. Chapelier[1,2], and M. Hofheinz[1,2]

[1] *Univ. Grenoble Alpes, INAC-PhElIQS, F-38000 Grenoble, France.*
[2] *CEA, INAC-PhElIQS, F-38000 Grenoble, France. and*
[3] *Univ. Grenoble Alpes, SIMAP, F-38000 Grenoble, France.*

(Dated: April 1, 2016)

Niobium nitride (NbN) is widely used in high-frequency superconducting electronics circuits because it has one of the highest superconducting transition temperatures ($T_c \sim 16.5$ K) and largest gap among conventional superconductors. In its thin-film form, the T_c of NbN is very sensitive to growth conditions and it still remains a challenge to grow NbN thin film (below 50 nm) with high T_c. Here, we report on the superconducting properties of NbN thin films grown by high-temperature chemical vapor deposition (HTCVD). Transport measurements reveal significantly lower disorder than previously reported, characterized by a Ioffe-Regel ($k_F \ell$) parameter of ~ 14. Accordingly we observe $T_c \sim 17.06$ K (point of 50 % of normal state resistance), the highest value reported so far for films of thickness below 50 nm, indicating that HTCVD could be particularly useful for growing high quality NbN thin films.

Niobium nitride (NbN)thin films — thanks to their high $T_c \sim 16.5$ K, superconducting energy gap $\Delta \sim 2.5$ meV, and upper critical field $B_{c2} \sim 40$ T — have been the subject of intense research for the last few decades, both on application and fundamental grounds. The combination of high T_c and small coherence length ($\xi(0) \sim 5$ nm) allows one to fabricate very thin NbN films with reasonably high T_c, which is essential for, e.g, Superconducting Single Photon Detectors (see e.g.[1, 2]). NbN thin films are used as hot electron bolometers and superconducting radio frequency cavities. NbN has higher kinetic inductance to other S-wave superconductors[3], which this helps fabricating superconducting micro wave resonators with high characteristic impedance and microwave kinetic inductance detectors. On the fundamental level, the effects of disorder on superconducting and normal state properties have been studied in NbN thin films [4–6]. Nano-wires, made from NbN thin films, have demonstrated thermal and quantum phase slips [7]— a phenomenon of great interest in understanding one-dimensional superconductivity. Further, the large superconducting energy gap of NbN can be explored in designing circuit Quantum Electrodynamics experiments in the THz frequency range.

Thus, there has been a growing demand of high quality NbN thin films. Reactive DC magnetron sputtering from an Nb target in an argon and nitrogen atmosphere is most commonly used to deposit NbN on various substrates[8–10]. The main difficulty in this process, arises from the creation of atomic level nitrogen vacancies and from the formation of non-superconducting Nb_2N and hexagonal phases. Besides, in the optimal parameter range, the high sputtering rate (typically $\sim$ 1-5 nm/sec) makes it difficult to control the thickness below 10 nm. Some other methods, where the superconducting properties of NbN thin films were probed, include Pulsed Laser Deposition (PLD) [11, 12], Molecular Beam Epitaxy (MBE) [13] and Atomic Layer Deposition (ALD) [14]. In this regard, deposition of superconducting NbN films by high temperature chemical vapor deposition (HTCVD) is rather rare. HTCVD, compared to most of the other methods, has certain advantages: it is cost effective, especially for large scale productions and the growth rate being tunable to low values (down to 1 nm/minute), it is easy to control the thickness of the films.

A first step to explore HTCVD as an alternative to the existing methods to produce good quality superconducting NbN films, we grow three 40-nm thick NbN films by HTCVD, and investigate their superconducting properties. The free electron density (n) of the films is determined from Hall measurements at room temperature. The zero temperature upper critical field $B_{c2}(0)$ and the Ginzburg-Landau coherence length $\xi(0)$ are estimated from magneto resistance data near T_c. The strong coupling nature of our NbN films is confirmed by superconducting energy gap (Δ) measurement of a film by scanning tunnel spectroscopy at 1.35 K. We also estimate $\lambda(0)$ from the normal state resistivity (ρ_{xx}) and $\Delta(0)$. Our best film has very high $k_F \ell \sim 14$ and $T_c \sim 17.06$ K, and quite low $\rho_{xx} \sim 60$ $\mu\Omega$cm and $\lambda(0) \sim 175$ nm, making it very promising for many superconducting applications.

I. EXPERIMENTS AND RESULTS

Three 40-nm-thick NbN films, labeled as S2, S3, and S4 respectively, were grown simultaneously (under the same process condition) at 1300 °C on different sapphire substrates by HTCVD. The detailed deposition process and the structural characterizations of the films are reported elsewhere [15]. Briefly, S2 and S4 were grown on ($11\bar{2}0$) and (0001) oriented sapphire (Al_2O_3) substrate, respectively; whereas, S3 was grown on (0001) orientated Al_2O_3 with a buffer layer of 80-nn-thick aluminium nitride (AlN) buffer layer grown by HTCVD [16]. X-ray diffraction and HRTEM studies reveal that all the NbN-
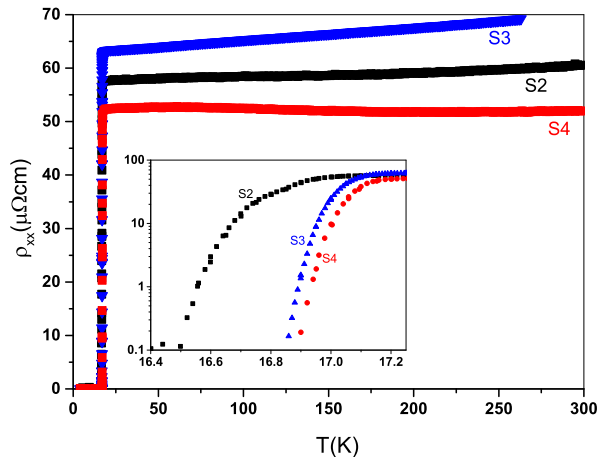
FIG. 1. The temperature variation of resistivity (ρ_{xx}) for S2, S3, and S4. The inset shows a zoom on the superconducting transition. The ρ_{xx} at 17.25 K, T_c, and ΔT_c are listed in Table I.
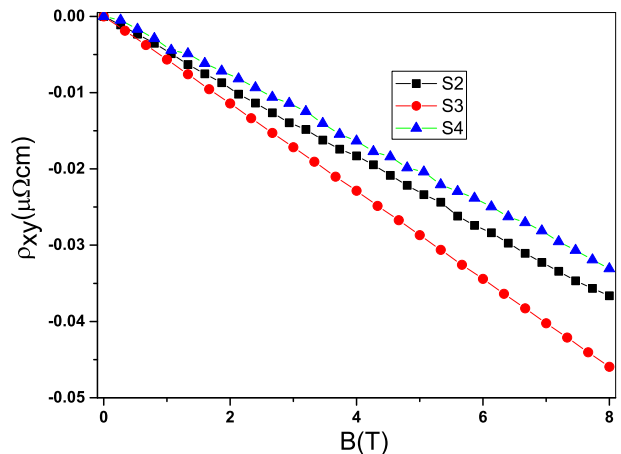

FIG. 2. The hall resistivity for all three samples at room temperature. The magnetic field was scanned from 0 to 8 T. The electron densities, listed in Table-I, are estimated from the slope (R_H) using the formula: $R_H = 1/ne$.

films contain face centered cubic (FCC) as primary phase, grown preferentially along the (111) orientation. The average out-of-plane lattice parameters (a) are listed in Table I. Apart from the (111) preferential orientation, all the films also show additional orientations (mainly 200). The f factors — a measure of the degree of preferential orientation for FCC films [17] — are also listed in Table I. S2, apart from containing only cubic phases, does not contain any other phase; whereas S3 and S4 also contain a very small fraction of hexagonal phases, more in S3 than in S4.

The electrical transport measurements were performed down to 4 K in a commercial physical property measurement system (PPMS). In Fig. 1, we plot the temperature variation of resistivity (ρ_{xx}) for S2, S3, and S4. In the normal state, the resistivity has very little variation in temperature. The normal state resistivities ρ_{xx} of the films, defined at T = 17.25 K, are listed in Table I. The inset of Fig. 1 shows the superconducting transition of resistivity (on a log scale). The T_c of the films, defined as the temperatures where resistivity is half of the normal value, are listed in Table I.

In Fig. 2, we plot the Hall resistivity (ρ_{xy}) for all three samples. The electron density (n) was estimated from the slope, known as the Hall resistance $R_H = 1/ne$, where e is the charge of an electron. The Hall measurement was performed at room temperature where electron–electron interaction is expected to be weak [18], justifying the free electron approximation. R_H values at room temperature for all three samples are listed in Table I. Knowing n and ρ_{xx}, the elastic scattering time (τ) was estimated from Drude's formula: $\rho_{xx} = m/ne^2\tau$, here, m is the mass of a free electron. The other important parameters — the Fermi wave vector(k_F), the Fermi velocity (v_F), the mean free path (ℓ), and the diffusion constant (D) — were estimated from the following formulae: $k_F = (3\pi^2 n)^{1/3}$,

$v_F = \hbar k_F/m$, $\ell = v_F\tau$, $D = v_F\ell/3$. In Table II, we summarize these parameters together with $k_F\ell$.

In Fig. 3, we present the magneto-resistance data for S3. Fig. 3a presents the variation of ρ_{xx} as a function of temperature for magnetic fields from 0 to 8 T. The graph clearly shows that the zero temperature value of the upper critical field ($B_{c2}(0)$) is greater than 8 T, the maximum field our set up could provide. We, therefore, extract $B_{c2}(0)$ from the following formula: $B_{c2}(0) = 0.69T_c\left|\frac{dB_{c2}}{dT}\right|_{T=T_c}$ [19]. The slope near T_c, $\left(\frac{dB_{c2}}{dT}\right)_{T=T_c}$, was extracted as shown in Fig.3b. Here, we plot the variation of resistance as a function of magnetic field at different temperatures near T_c. The inset shows the variation of B_{c2}, defined as the field where the resistivity is half the normal state value of ρ_{xx} (taken at 17.25 K), as a function of temperature. The slope is extracted from the straight line fit, indicated by the solid line. We also extract $\xi(0)$ from the slope, using the following formula: $\xi(0) = \sqrt{\Phi_0/2\pi T_c \left|\frac{dB_{c2}}{dT}\right|_{T=T_c}}$ [20]. In Table-II, we summarize both $B_{c2}(0)$ and $\xi(0)$.

In order to estimate the zero temperature superconducting energy gap ($\Delta(0)$) of our films, we have performed scanning tunneling spectroscopy (STS) measurement on S2 at T = 1.35 K, a temperature much lower than T_c. $\Delta(0)$ is found to be inhomogeneous over space— its value ranging from 2 meV to 2.8 meV. The suppressed superconducting gaps might be due to local contamination or oxidation of the surface as the sample had been exposed to air over a period of more than one year prior to STS measurements . Fig. 4 shows an experimental spectrum and a fit computed with a gap of 2.8 meV according to Bardeen-Cooper-Schrieffer (BCS)[21] theory. This leads to a ratio 2 Δ / $k_B T_c = 4$, which is slightly less than values reported in the literature [6, 10].

TABLE I. Summary of the experimental results. Here, ρ_{xx} is the normal state resistivity at $17.25\,\mathrm{K}$. T_c is defined at a temperature where resistivity is half of ρ_{xx}.

Samples	Substrate	a	f factor	R_H	ρ_{xx}	T_c	ΔT_c	$\left.\frac{\mathrm{d}B_{c2}}{\mathrm{d}T}\right|_{T=T_c}$
		Å		$(10^{-3}\mu\Omega\mathrm{cm/T})$	$(\mu\Omega\mathrm{cm})$	(K)	(K)	(T/K)
S2	Al$_2$O$_3$ (1120)	4.436	0.92	4.6	57.1	16.80	0.55	0.96
S3	AlN (0001)	4.434	0.99	5.6	62.5	17.02	0.32	0.99
S4	Al$_2$O$_3$ (0001)	4.427	0.98	4.1	51.3	17.06	0.32	0.96

TABLE II. Summary of the various parameters calculated from the experimental results of Table I.

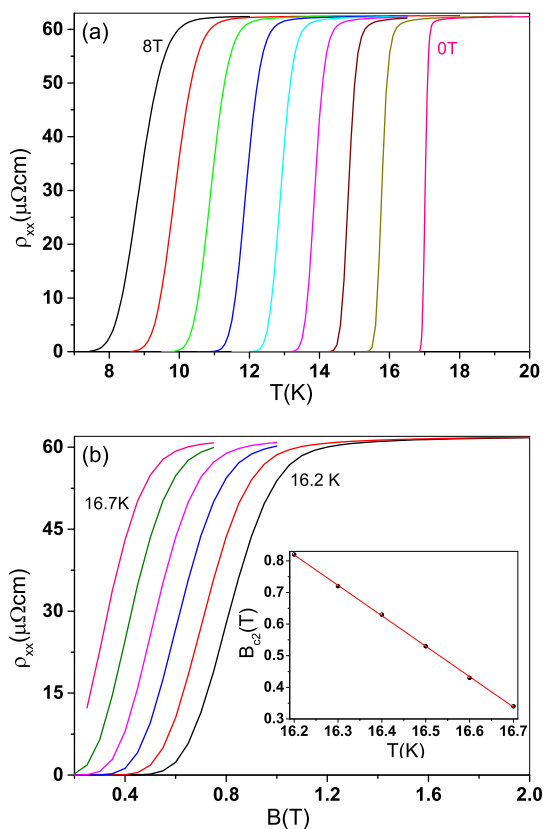| Samples	n	τ	ℓ	D	$k_F\ell$	N_u	$B_{c2}(0)$	$\xi(0)$	$\lambda(0)$
	$(10^{29}/\mathrm{m}^3)$	(fS)	(nm)	$(\mathrm{cm}^2/\mathrm{sec})$		$((\mathrm{eV})^{-1})$	(T)	(nm)	(nm)
S2	1.34	0.46	0.84	5.1	13	0.46	11.1	6.5	179
S3	1.10	0.52	0.89	5.1	13	0.43	11.3	6.5	186
S4	1.49	0.46	0.87	5.5	14	0.48	11.7	6.4	169

FIG. 3. (a) The variation of resistivity (ρ_{xx}) of S3 as a function of temperature for magnetic fields 0 to $8\,\mathrm{T}$. (b) The variation of ρ_{xx} as a function of magnetic field at different temperatures, 16.2 to $16.7\,\mathrm{K}$ with increments of $0.1\,\mathrm{K}$, near T_c. The inset shows the variation of the B_{c2} as a function of temperature, with B_{c2} being defined as the field where the resistance is half of the normal state resistance at $17.25\,\mathrm{K}$. The straight line fit, indicated by the solid line, gives the slope used to determine $B_{c2}(0)$ and $\xi(0)$, listed in Table II.

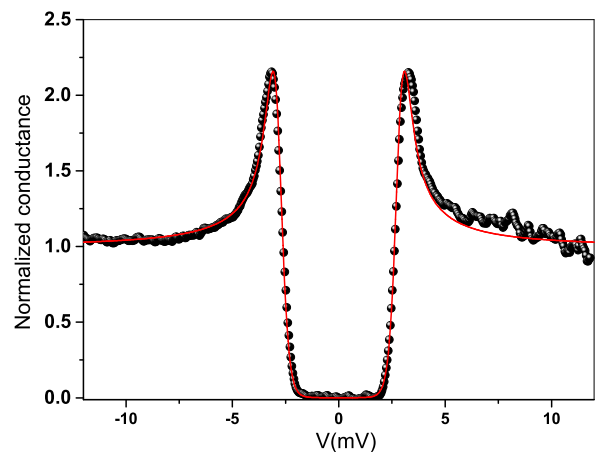FIG. 4. Normalized tunneling conductance versus bias voltage at $1.35\,\mathrm{K}$ on sample S2 (black points). The red curve is a BCS theoretical fit with a superconducting gap of $2.8\,\mathrm{meV}$.

II. ANALYSIS AND DISCUSSION

We have, so far, extensively used free electron model (FEM) to estimate various parameters like n or $k_F\ell$. FEM, in general, works very well for good metals. On the other hand, unlike a good metal, our films have very little variation in resistivity as a function of temperature in the normal state (Fig. 1). Thus, it is not obvious that the free electron model should work well. In this regard, we observe that the free electron densities n of our films are significantly lower than the theoretical estimate of $n = 2.39 \times 10^{29}/\mathrm{m}^3$[22]. The other important parameter to compare, as suggested by Chockalingam et. al [10], is the density of state (DOS) at the Fermi level. The DOS per unit volume per energy level, in the framework of free electron model, is given by: $N_V = mk_F/\hbar^2\pi^2$. The DOS per NbN unit, N_u, listed in Table-I, is then $N_u = N_V a^3/4$ (each unit cell of volume a^3 is shared by 4 NbN units). Contrary to the electron density n, we

see that the estimated DOSs are quite close to the theoretical estimate of 0.54/eV [23] or from the specific heat measurement $\approx 0.5/$eV [24].

The critical temperature $T_c \sim 17$ K of our films is, to the best of our knowledge, the highest reported to date for NbN thin films with thickness 50 nm or less. The T_c values stated in Table-I are defined as the point of 50% of the normal state resistance (taken at 17.25 K). The resistivity reaches 1% of the normal state resistance at 16.60 K, 16.89 K, and 16.91 K for S2, S3, S4, respectively. These numbers are still significantly higher than previously reported numbers and show that the superconducting transition is very sharp. This, we believe, is the result of the epitaxial nature and therefore the good crystallinity of our films, that lead to $k_F\ell$ values significantly higher than the ones reported previously (see e.g., [10, 25]). Chand et al.[25] reported $T_c \sim 17.0$ K for one of their sputtered NbN films with thickness more than 50 nm. For sputtered NbN films, the enhancement of T_c with thickness has been observed even above 100 nm [9]. Chockalingam et al. [10] also observed a systematic increase in T_c with n or DOS at the Fermi level. We do not observe such trend. Wang et al. [9] observed a systematic non-monotonic variation of T_c with a; the highest T_c, they observed, was for $a = 4.46$ Å.

The upper critical field B_{c2} is very similar for all of our films, but much lower than for other films with T_c higher than 14 K reported in the literature[10, 26, 27]. In the dirty limit — defined by $\ell \ll \xi(0)$ — $B_{c2}(0)$ is related to resistivity and diffusion constant via $B_{c2}(0) = 0.69T_c4k_B/\pi eD = 0.69T_c4ek_BN_V\rho_{xx}/\pi$ [28]. The low B_{c2} are, therefore, a further indication that our films have lower disorder, i.e. larger diffusion constant / lower resistivity. Indeed, the resistivities $\rho_{xx} \sim 60\,\mu\Omega$cm we observe are significantly lower than previously reported [10, 26, 27]. One should note, however, that the above formula yields $B_{c2}(0) \sim 2.5$ T for our films, a significantly lower field than the value extracted from Fig. 3.

This discrepancy could be due to the spin-orbit interaction, which has not been taken into account in the above formula and can enhance $B_{c2}(0)$ very significantly [29].

Finally, we estimate the zero temperature value of the magnetic penetration depth ($\lambda(0)$) from $\Delta(0)$, using the following formula [30]: $\lambda^{-2}(0) = \pi\mu_0\Delta(0)/\hbar\rho_{xx}$. For NbN films, this formula is found to closely match experiment [30]. The calculated $\lambda(0)$s are listed in Table-I. In our calculation, $\Delta(0)$ is estimated from strong coupling relation $2\Delta(0)/k_BT_c = \alpha$ — assuming $\alpha = 4.00$ for all three films. S4, as we see from Table-I, has minimum $\lambda(0)$ among three films, which is due to its highest T_c and lowest ρ_{xx} values.

In summary, we have found exceptionally high critical temperatures around 17 K and large superconducting gap of 2.8 meV for NbN films grown by HTCVD at 1300 °C on sapphire and AlN. We explain this high critical temperature by very large $k_F\ell$ parameters indicating low disorder. Consistent with this interpretation, we observe low resistivity ($\sim 60\,\mu\Omega$cm) and low upper critical field ($\sim$11 T). Our results demonstrate that HTCVD, a particularly cost effective growth technique, is a very promising alternative to magnetron sputtering for depositing high-quality NbN thin films. A natural extension of this work will be to to further investigate the existing links between the material characteristics and the superconducting properties and to explore the limits of the HTCVD techniques for the production of high quality ultra thin films of NbN.

[1] Delacour, C.; Claudon, J.; Poizat, J. P.; Pannetier, B.; Bouchiat, V.; Espiau de Lamaestre, R.; Villegier, J.-C.; Tarkhov, M.; Korneev, A.; Voronov, B.; Goltsman, G. Appl. Phys. Lett. **90**, 191116 (2007).

[2] G. Goltsman, A. Korneev, A. Divochiy, O. Minaeva, M. Tarkhov, N. Kaurova, V. Seleznev, B. Voronov, O. Okunev, A. Antipov, K. Smirnov, Yu. Vachtomin, I. Milostnaya, and G. Chulkova, J. Mod. Opt. **56**, 1670 (2009).

[3] Anthony J Annunziata, Daniel F Santavicca, Luigi Frunzio, Gianluigi Catelani, Michael J Rooks, Aviad Frydman and Daniel E Prober, Nanotechnology **21**, 445202 (2010).

[4] M. Mondal, S. Kumar, M. Chand, A. Kamlapure, G. Saraswat, G. Seibold, L. Benfatto, and P. Raychaudhuri, Phys. Rev. Lett. **107**, 217003 (2011).

[5] M. Chand, G. Saraswat, A. Kamlapure, M. Mondal, S. Kumar, J. Jesudasan, V. Bagwe, L. Benfatto, V. Tripathi, and P. Raychaudhuri, Phys. Rev. B **85**, 014508 (2012).

[6] Y. Noat, V. Cherkez, C. Brun, T. Cren, C. Carbillet, F. Debontridder, K. Ilin, M. Siegel, A. Semenov, H.-W. Hbers, and D. Roditchev, Phys. Rev. B **88**, 014503 (2013).

[7] C. Delacour, B. Pannetier, J. C. Villegier, and V. Bouchiat, Nano Lett.**12**, 3501 (2012).

[8] J. R. Gavaler, J. K. Hulm, M. A. Janocko and C. K. Jones, , J. Vac. Sci. Technol. **6**, 177 (1969)

[9] Z. Wang, A. Kawakami, Y. Uzawa, and B. Komiyama, J. Appl. Phys. **79**, 7837 (1996).

[10] S. P. Chockalingam, M. Chand, A. Kamlapure, J. Jesudasan, A. Mishra, V. Tripathi, and P. Raychaudhuri, Phys. Rev. B **77**, 214503 (2008).

[11] R. E. Treece, M. S. Osofsky, E. F. Skelton, S. B. Qadri, J. S.Horwitz and D. B. Chrisey, Phys. Rev. B **51** 9356

(1995); R.E. Treece, J. S. Horwitz, J. H. Classen and D. B. Chrisey, Appl. Phys. Lett.**65** 2860 (1994).

[12] K. Senapati, N. K. Pandey, Rupali Nagar, and R. C. Budhani, Phys. Rev. B **74**, 104514 (2006).

[13] S.-Z. Lin, O. Ayala-Valenzuela, R. D. McDonald, L. N. Bulaevskii, T. G. Holesinger, F. Ronning, N. R. Weisse-Bernstein, T. L. Williamson, A. H. Mueller, M. A. Hoffbauer, M. W. Rabin, and M. J. Graf, Phys. Rev. B **87**, 184507 (2013).

[14] Mario Ziegler, Ludwig Fritzsch, Julia Day, Sven Linzen, Solveig Anders, Julia Toussaint and Hans-Georg Meyer, Supercond. Sci. Technol.**26**, 025008 (2013).

[15] Mercier, Frdric, Stphane Coindeau, Sabine Lay, Alexandre Crisci, Matthieu Benz, Thierry Encinas, Raphal Boichot et al. Surface and Coatings Technology, **260**, 126 (2014).

[16] R. Boichot, N. Coudurier, F. Mercier, S. Lay, A. Crisci, S. Coindeau, A. Claudel, E. Blanquet, M. Pons, Surface and Coatings Technology, **237**, 118 (2013).

[17] E.F. Skelton, S.A. Wolf, and T.L. Francavilla, J. Vac. Sci. Technol. **18 (2)** 259 (1981); For an ideal epitaxial FCC film f-factor should be 1. We can, therefore, say that S3 is the most epitaxial and S2 is the least epitaxial among three films.

[18] M. A. Khodas and A. M. Finkelstein, Phys. Rev. B **68**, 155114 (2003).

[19] E. Helfand and N. R. Werthamer, Phys. Rev. **147**, 288 (1966).

[20] M. Tinkham, Introduction to Superconductivity 2nd ed. (Mc Graw-Hill, New York, 1996).

[21] J. Bardeen, L. N. Cooper and J. R. Schrieffer, Phys. Rev. **108** , 1175 (1957).

[22] M. P. Mathur, D. W. Deis, and J. R. Gavaler, J. Appl. Phys. **43**, 3158 (1972).

[23] L. F. Mattheiss, Phys. Rev. B **5** , 315 (1972).

[24] T. H. Geballe, B. T. Matthias, J. P. Remeika, A. M. Clogston, V.B. Compton, J. P. Maita, and H. J. Wiliams, Physics (Long Island City, N.Y.) **2**, 293 (1966).

[25] M. Chand, G. Saraswat, A. Kamlapure, M. Mondal, S. Kumar, J. Jesudasan, V. Bagwe, L. Benfatto, V. Tripathi, and P. Raychaudhuri, Phys. Rev. B **85**, 014508 (2012).

[26] D. W. Capone II, K. E. Gray, and R. T. Kampwirth, J. Appl. Phys. **65**, 258 (1989).

[27] Garima Saraswat, Priti Gupta, Arnab Bhattacharya, and Pratap Raychaudhuri APL Mater. **2** 056103 (2014).

[28] P. G. DeGennes, Superconductiuity of Metals and Alloys, (Benjamin, New York, 1966).

[29] N. R. Werthamer, E. Helfland, and P. C. Honenberg, Phys. Rev. **147**, 295 (1966).

[30] A. Kamlapure, M. Mondal, M. Chand, A. Mishra, J. Jesudasan, V. Bagwe, L. Benfatto, V. Tripathi, and P. Raychaudhuri, Appl. Phys. Lett. 96, 072509 (2010).
L. Mechin, M. P. Chauvat, and P. Ruterana, IEEE TRANSACTIONS ON APPLIED SUPERCONDUCTIVITY, **19**, NO. 3, JUNE 2009.